



Kent Academic Repository

Dui, Hongyan, Liu, Kaixin and Wu, Shaomin (2023) *Cascading failures and resilience optimization of hospital infrastructure systems against the COVID-19*. *Computers & Industrial Engineering*, 179 . ISSN 0360-8352.

Downloaded from

<https://kar.kent.ac.uk/100575/> The University of Kent's Academic Repository KAR

The version of record is available from

<https://doi.org/10.1016/j.cie.2023.109158>

This document version

Author's Accepted Manuscript

DOI for this version

Licence for this version

CC BY-NC-ND (Attribution-NonCommercial-NoDerivatives)

Additional information

Versions of research works

Versions of Record

If this version is the version of record, it is the same as the published version available on the publisher's web site. Cite as the published version.

Author Accepted Manuscripts

If this document is identified as the Author Accepted Manuscript it is the version after peer review but before type setting, copy editing or publisher branding. Cite as Surname, Initial. (Year) 'Title of article'. To be published in **Title of Journal** , Volume and issue numbers [peer-reviewed accepted version]. Available at: DOI or URL (Accessed: date).

Enquiries

If you have questions about this document contact ResearchSupport@kent.ac.uk. Please include the URL of the record in KAR. If you believe that your, or a third party's rights have been compromised through this document please see our [Take Down policy](https://www.kent.ac.uk/guides/kar-the-kent-academic-repository#policies) (available from <https://www.kent.ac.uk/guides/kar-the-kent-academic-repository#policies>).

Cascading failures and resilience optimization of hospital infrastructure systems against the COVID-19

Hongyan Dui^a, Kaixin Liu^a, Shaomin Wu^b

^aSchool of Management, Zhengzhou University, Zhengzhou 450001, China

^bKent Business School, University of Kent, Canterbury, Kent CT2 7FS, UK

Abstract: The outbreak of the Coronavirus Disease 2019 (COVID-19) has put the resilience of a country's healthcare infrastructure to the most severe test. The challenge of taking emergency measures to optimize the supply of medical resources and effectively meet the medical needs of residents is an important issue that needs to be resolved urgently in the prevention and control of public health emergencies. This paper analyzes cascading failures and optimization of the resilience of the hospital infrastructure system (HIS) with the presence of the COVID-19. It proposes a propagation model to describe the COVID-19 infectious process and establishes a cascading failure model of a HIS to analyze its failure mechanism. It also proposes a method for optimizing the resilience of HIS. Then the supplies and demands in maintaining the operations of HIS are studied, and a restoration strategy is obtained. Finally, simulation analysis of the spread of the COVID-19 is carried out to illustrate the applicability of the proposed method.

Keywords: reliability; cascading failure; resilience; hospital infrastructure system; supply chain

1. Introduction

1.1. Background

In December 2019, a coronavirus disease, which was later named as the COVID-19, was detected in Wuhan, Hubei Province, China, and then began spreading globally. It is transmitted mainly by respiratory droplets and physical contact and is highly contagious. It poses a tremendous threat to the lives and people's health, and causes immense damage to economic and social development. As of 12:02 am, February 28, 2023 (Greenwich time), there are 679,887,320 COVID-19 infected cases and 6,799,660 deaths relating to the

26 COVID-19 (Worldometer, 2023). The World Health Organization has listed the COVID-19 as a public health
27 emergency of international concern.

28 As the main part of a healthcare system for responding public health emergencies, hospital
29 infrastructure systems (HIS's) are directly responsible for the prevention and control of epidemics. A HIS is
30 a complex system composed of medical staff and various types of medical resources interacting with each
31 other and can be abstracted as a complex network consisting of all hospitals and their linkage relationships.

32 At the beginning of the outbreak of the COVID-19, hospitals were overwhelmed with COVID-19
33 patients and HIS's struggled in coping with the surging medical demand. The outbreak of the COVID-19
34 put the resilience of HIS's to the test, and emergency management tools were therefore necessary in
35 managing the performance and quantity of medical resources. To address the shortcomings and deficiencies
36 revealed in the outbreak of the COVID-19, there is a need to conduct failure analysis of HIS's and investigate
37 post-disaster restoration strategies for HIS's. This paper serves this purpose.

38 **1.2. Literature reviews**

39 The infectious disease dynamics model (IDD model) is an effective tool for the study of infectious
40 diseases, on which there is an abundance of work (Gao & Wang, 2022; Qian & Ukkusuri, 2021; Kermack &
41 Mckendrick, 1927; Gao, Liu, Nieto & Andrade, 2011; Enatsu, Messina, Nakata, Muroya, & Vecchio, 2012).
42 In the literature, there are two main approaches to characterizing the dynamics of infectious diseases: the first
43 one includes compartmental models and the second one models the disease propagation at the individual level
44 over large-scale networks (Qian & Ukkusuri, 2021). Particularly, a compartmental model classifies the
45 population under study into several states: susceptible (S), latent (E), infected (I), and recovered (R). The
46 transition between the states of the subjects describes the process of virus propagation. A susceptible person,
47 as a latent person, could be contracted by an infected person, which may then become a recovered one after
48 being treated. Compartmental models include SIR (susceptible-infected-recovered) models, SIRS (susceptible-

49 infected-recovered-susceptible) models, SEIR (susceptible-exposed-infected-removed) models, among others.
50 Kermack & Mckendrick (1927) first proposed the SIR model in 1927, assumed that the number of people in
51 the target area was constant and that people recovered from the virus will no longer infected, and divided the
52 target population into three categories: susceptible (S), infected (I), and recovered (R). Enatsu, Messina, Nakata,
53 Muroya, & Vecchio (2012) and Sekiguchi & Ishiwata (2010) studied discrete-time SIRS infectious disease
54 kinetic models with time lags and non-linear incidence. They used mathematical induction, the principle of
55 comparison of differential equations and the construction of appropriate Lyapunov functions, to obtain the
56 conclusion that the disease is persistent when the underlying regeneration number is greater than one.

57 Researchers have proposed complex network virus models based on compartmental models, and they
58 treat individuals as nodes and connections between individuals as node-linked edges to study the virus
59 propagation process on both homogeneous and non-homogeneous networks. Gagliardi & Alves (2010) studied
60 the effect of small-world effect on virus propagation based on Cellular Automata (CA) and concluded that
61 enhanced network small-world effect can accelerate the virus propagation rate, etc. Wang, Wang, Liu & Li
62 (2014) studied an SIR epidemic model with demographics and time-delay on networks. According to Zhang
63 & Jin (2011), the epidemic model has been considered networks with birth and death rates, where the basic
64 reproductive threshold parameter is defined to show the dynamics of an epidemic.

65 Most of the research on the cascading failures in a complex network has focused on quantitative analysis
66 and applied research (Sheu et al., 2020; Whitman et al., 2017). Wang & Xiao (2016) presented a cascade
67 failure model based on an improved ant colony algorithm for a cluster-distributed supply chain network, taking
68 into account the topology of the network, the flexibility of the nodes and the efficiency of the nodes. Zhou,
69 Huang, Coit & Fel (2018) analyzed the process of network cascade failures from the perspectives of load
70 dynamics and node dependence, respectively. Zheng, Gao & Zhao (2007) constructed a cascade failure model
71 for scale-free networks that consider aggregation coefficients and congestion effects, and pointed out the

72 characteristics of network element coefficients with high sensitivity to failures. Rodríguez-Méndez, Ser-
73 Giacomini & HernándezGarcía (2017) investigated the characteristics of clustering coefficients in the cascade
74 failure process of fluid networks and the impact on the scale of its failures. Linkov, Keenan & Trump (2021)
75 reviewed research that applies risk, resilience, and strategy theories to civil, environmental, and public health
76 in the context of COVID-19. Their work enables decision-makers to understand the systemic and sweeping
77 nature of the COVID-19 pandemic. Hynes, Trump, Love & Linkov (2020) point out that COVID-19 can reduce
78 the ability of critical systems to withstand shocks and can cause failures in one system to spread to another.
79 Wells, Boden, Tseytlin & Linkov (2022) conducted a literature review on the resilience of critical infrastructure
80 in the network science literature published between 2010 and 2021 under compounding failure. Guo et al.
81 (2019) developed a cascade model that takes account of the project's self-protection mechanism to examine a
82 failure propagation process originated from a single task failure.

83 There are many studies on maintenance optimization of complex systems (Broek, Teunter, Jonge &
84 Veldman, 2021; Broek, Teunter, Jonge & Veldman, 2019; Keizer, Teunter & Veldman, 2017; Zhao et al., 2018),
85 and resilience is an indicator to guide the maintenance of complex systems (Almoghathawi and Barker, 2019).
86 The word "resilience" is originally derived from the Latin word "resiliere", meaning "to rebound", and is
87 commonly used to indicate *the ability of a system to sustain external and internal disruptions without*
88 *interrupting the execution of system functions, or, if the function is disconnected, to fully recover the function*
89 *rapidly* (Hosseini, Barker & Ramirez-Marquez, 2016). Galaitsi et al. (2021) studied eight concepts, which
90 characterize systems facing threats: adaptability, agility, reliability, resilience, resistance, robustness, safety,
91 security, and sustainability. They found that resilience could only manifest when recovery is needed, and thus
92 could complement concepts related to threat impact like resistance, robustness, safety, and security. Siskos &
93 Burgherr (2022) proposed an elaborative multicriteria decision support methodological framework for the
94 Evaluation of Electricity Supply Resilience, based on three major resilience dimensions including "resist",

95 “restabilise” and “recover”. Ouyang (2017) proposed a mathematical framework to support resilience
96 optimization of interdependent critical infrastructure system under the worst critical infrastructure system.
97 Linkov et al. (2018) proposed a three-tier qualitative analysis framework for resilience assessment. The
98 framework allows regulators to integrate resilience assessments with existing risk assessment protocols.
99 Ransolin, Saurin and Formoso (2020) developed a framework for the integrated modelling of built environment
100 and functional requirements, supporting the analysis of resilient performance.

101 In the context of HIS’s, resilience refers to its ability to recover quickly from an attack by a health event.
102 The continued operation of infrastructure is fundamental to people’s daily life, and optimizing the resilience
103 of Hospital Infrastructure Systems is essential for the safety and health of the population (Barabadi, Ghiasi &
104 Nouri, 2020). Studies on HIS resilience under emergencies can be found in the literature. Pishnamazzadeh,
105 Sepehri & Ostadi (2020) proposed a model to assess hospital resilience based on a system dynamics approach.
106 The model studied the effect of four Key Performance Indicators (KPI) of hospitals: patient satisfaction, patient
107 waiting time, staff burnout and staff satisfaction on the resilience. Achour, Miyajima, Pascale & Price (2014)
108 assessed the resilience of healthcare institutions under supply disruption, using data from hospitals in the
109 aftermath of the 2003 Tohoku earthquake in Japan for validation. Tariverdi, Fotouhi, Moryadee & Miller-
110 Hooks (2018) proposed a hierarchical modeling concept to quantify the resilience of regional hospital response
111 under disaster, and estimated resilience in terms of total patient waiting time and unserved patients. Zhang,
112 Shi, Huang, Hua & Teunter (2021) studied policies for optimizing the inventory and capital reserves of
113 emergency medical resources under the COVID-19. Samsuddin, Takim, Nawawi & Alwee (2018) measured
114 hospital’s disaster resilience as the hospital’s ability to resist, absorb, accommodate and recover from the
115 effects of a hazard in a timely and efficient manner. Additionally, they investigated the hospital preparedness
116 attributes and resilience indicators and established relationship of preparedness attributes towards hospital’s
117 resilience. Hassan and Mahmoud (2021) investigated the combined impact of wildfire and pandemic on a

118 network of hospitals, they combined wildfire data with varying courses of the spread of COVID-19 to evaluate
119 the effectiveness of different strategies for managing patient demand. Li et al. (2020) developed a system
120 dynamics model describing hospital functionality after earthquakes (SD-HFE) to simulate hospital
121 functionalities, then the resilience assessment can then be conducted based on the functionality curve. Grimaz,
122 Ruzzene & Zorzini (2021) illustrated the RADAR-HF (Recon Analysis for Detecting the Actual situation and
123 the improvement Requests, applied to Hospital Facilities) developed for the situational assessment of the
124 physical environment of hospital facilities. Decision makers can use RADAR-HF to define comprehensive
125 modernization strategies with resilience improvements, monitor the condition of facilities, and understand the
126 effectiveness of interventions. Barasa, Mbau and Gilson (2018) performed a systematic review of empirical
127 literature on organizational resilience, and made several observations that were relevant to nurturing the
128 resilience of health systems.

129 **1.3. Knowledge gaps, novelty and contributions**

130 From the above literature review, there are some hospital resilience models that apply resilience theory in
131 hospital management. There are four main categories of hospital resilience models in the literature: models
132 based on a system dynamics approach to studying the relevant factors affecting resilience, models that assess
133 resilience through different perspectives, models for optimizing resilience based on different optimization
134 purposes, and models that develop informative decision support systems. This paper presents a resilience
135 optimization model for hospitals based on a Markov decision process, which integrates the virus propagation
136 process and a hospital cascading failure process. Then a hospital resilience optimization model is proposed,
137 which can determine the restoration strategy of HIS's at each period and can restore the hospital's ability to
138 serve patients as soon as possible.

139 It can be seen from literature review that the resilience and COVID-19 has been studied from different
140 perspectives. However, there are some shortcomings in the above studies. First, studies on virus transmission

141 do not consider individual nodal heterogeneity. Second, the effect mechanism of virus propagation on the HIS
142 state is not considered. Third, an HIS is treated as a two-state system, however an HIS is a multi-state system.
143 Fourth, relevant studies did not investigate performing what restoration strategies for maximizing HIS
144 resilience in the event of cascading failure.

145 This paper aims to fill up these gaps and therefore makes the following contributions.

146 (a) We propose a COVID-19 propagation model with node heterogeneity based on the SEIR model. The
147 degree, activity capability and propagation capability of nodes are considered into the process of virus
148 propagation by nodes, the propagation probability of nodes is proposed to study the propagation process of
149 COVID-19 in the crowd based on SEIR model.

150 (b) The hospital cascading failure model is proposed by using the hospital outbreak rate as an indicator
151 of hospital cascading failures while taking into account the distribution of patient flow. This model can study
152 the influence mechanism of spread of the COVID-19 on the supply and demand in maintaining the operations
153 of hospital. In addition, the cascading model can also assess the loss to the hospital from the patient's
154 perspective.

155 (c) We apply the theory of resilience to manage HIS's and propose a quantitative framework for
156 resilience management. We propose a hospital resilience formula from the patient's perspective. The hospital
157 resilience is the ratio of the number of patients transferred out of the hospital to the number of patients
158 transferred in over a period of time, which can reflect the real-time resilience of the hospital and can quantify
159 the hospital's ability to serve patients unaffected by unexpected events.

160 (d) The paper considers a hospital as a polymorphic system and proposes an optimization model for HIS
161 resilience based on the Markov process. Real-time restoration strategies can be determined based on the
162 resilience optimization model.

163 1.4. Overview

164 This remainder of this paper is structured as follows. Section 2 proposes a COVID-19 propagation model
165 considering node heterogeneity and studies the propagation process of the disease. Section 3 proposes a
166 cascading failure model of a HIS under the COVID-19. Based on the load model, the cascading failure process
167 of a HIS is portrayed. Section 4 takes a hospital infrastructure network after a node failure as the object to
168 study the resilience optimization of HIS's under the COVID-19. Section 5 takes HIS's in two districts in a city
169 as an example for simulation verification. Section 6 wraps up the paper and proposes future research.
170 [Supporting Information](#) provides supplementary information on the Markov decision process modeling and
171 [some original data for simulation](#).

172 2. A COVID-19 propagation model based on node heterogeneity

173 2.1. Model indicators

174 Crowd is abstracted as a scale-free network, denoted by $G(V, W)$. Residents are abstracted as individual
175 nodes, denoted as V , and the connecting relationship between residents are abstracted as edges, denoted as W .
176 There are N nodes in the scale-free network, $V = \{1, \dots, i, \dots, N\}$, the element i in V represents the i -th node.
177 The adjacency matrix of $G(V, W)$ is represented by a matrix $[W_{ij}]_{N \times N}$, where $1 \leq i, j \leq N$, $W_{ij} = 1$, if node
178 i is connected to node j , $W_{ij} = 0$ otherwise.

179 Nodes with different attributes have different actions. Considering the heterogeneity of nodes, the
180 different attributes of nodes are described by a topological structure, activity ability and virus propagation
181 ability of crowd network nodes. The establishment indicators are as follows.

182 The degree of a node represents the structural centrality of the node and reflects the degree of mutual
183 influence between the node and its neighboring nodes. It represents the number of links between a node and
184 other nodes, and can reflect the number of people a person has contracted. The degree of node i is defined by:

$$185 F_i = \sum_{j=1}^N W_{ij}, \quad (1)$$

186 where W_{ij} is the adjacency relationship between node i and node j , N represents the number of nodes in
 187 $G(V, W)$, and F_i is the degree of node i .

188 The activity of a node is paroxysmal, and the activity time interval can describe its activity ability (Li,
 189 Guo, Gao, Zhang & Zhang, 2018). The higher level of physical activity of a node has, the higher possibility of
 190 the node participating in the virus spreading process has. If the node is a susceptible person with a high level
 191 of physical activity, the probability of the spread of infection of this person is higher. If the node is an infected
 192 person, the level of physical activity of the person is directly proportional to its ability to infect others. Inactive
 193 nodes do not perform any activities, such as spreading viruses and seeking medical treatment. At the end of
 194 each time interval, the node will have an active time point, at which the node can spread the virus. The activity
 195 time interval sequence of node i is $T_i = \{t_{i1}, t_{i2}, \dots, t_{iq_i}\}$, where $t_{iz}(z = 1, 2, \dots, q_i)$ follows a normal
 196 distribution, and q_i is the number of elements in T_i . The average value of the active time interval of node i is
 197 taken as the active time interval of node i . The level of physical activity A_i of node i is the ratio of the average
 198 value of the activity time interval of node i to the sum of the average value of the activity time interval of all
 199 nodes. A_i represents the activity capacity of individual node i related to the population, as shown in Eq. (2),

$$200 \quad A_i = -\ln \frac{\sum_{z=1}^{q_i} t_{iz}/q_i}{\sum_{i=1}^N (\sum_{z=1}^{q_i} t_{iz}/q_i)}. \quad (2)$$

201 The nodes in the crowd network are different. Therefore, different nodes are considered to have different
 202 virus propagation abilities. For the propagation of the COVID-19, the propagation ability P_i of node i is
 203 assumed constant. Let P_i be generated by a normally distributed random variable P , i.e., $P \sim N(\mu_p, \sigma_p^2)$, ($P_i =$
 204 0 when $P < 0$ and $P_i = 1$ when $P > 0$) (Zou, Towsley & Gong, 2004).

205 The level of physical activity of a node will affect its ability of the spread of infection. Nodes with a high
 206 level of physical activity can promote the spread of the virus more efficiently than those with a lower level of
 207 physical activity (Xin, Gao, Wang, Zhen & Li, 2019). The effective propagation ability of node i is $\sigma(i)$, as
 208 shown in Eq. (3),

209
$$\sigma_i = \begin{cases} P_i & A_i \geq a \\ 0 & 0 \leq A_i < a \end{cases} \quad (3)$$

210 where a is the average of the activity capacity of all nodes, P_i is the propagation ability of node i , A_i is the
 211 activity capacity of node i , and σ_i is the effective propagation ability of node i .

212 In the process of virus transmission, a person contracts the COVID-19 with a certain probability, and this
 213 probability is related to the number of people the person is exposed to and the effective transmission capacity
 214 of that person. The probability of transmission increases with the number of human contacts and the ability of
 215 effective transmission. Therefore, the propagation probability $\alpha(i)$ of node i can be expressed by

216
$$\alpha_i = \alpha_0 + \varepsilon F_i \sigma_i, \quad (4)$$

217 where α_0 is a given basic propagation probability, ε is a given parameter, and $0 < \alpha_i \leq 1$.

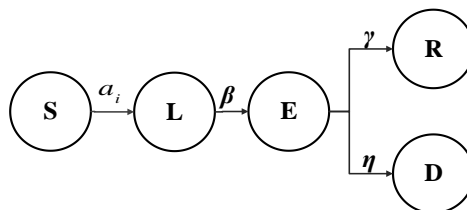
218 **2.2. The propagation model**

219 Combining the characteristics of the propagation process of COVID-19, the SEIR propagation model of
 220 COVID-19 is established. In the model, nodes have the following five states:

- 221 • Susceptible state S: The node has not yet been infected with the virus.
- 222 • Latent state L: The node has been infected by the virus and is asymptomatic but contagious.
- 223 • Exposed state E: The node has been infected by the virus, is symptomatic and contagious.
- 224 • Recovered state R: The node has recovered from COVID-19, is immune to further infection and is
 225 incontinentuous.
- 226 • Dead state D: The node has died with COVID-19 and is incontinentuous.

227 We take the crowd network as the object to establish a COVID-19 propagation model, as shown in Fig.

228 1.



229 Fig. 1. The COVID-19 propagation model
 230

231 Assume that the existence of edges between nodes is a condition for the realization of virus propagation,
 232 and nodes transferred to both cured and dead states will no longer participate in the network propagation
 233 process. Therefore, the state transition rules of nodes are as follows.

234 In this paper, time is divided into identical periods. The states of individuals and hospital nodes in each
 235 period will be studied, with k denoting the order of a period in the following. In each period, a susceptible
 236 state node i is infected by its neighboring nodes with probability α_i , and then transitions to the latent state,
 237 which has the onset symptom with probability β and then transitions into the exposed state. The exposed state
 238 node will be cured in the hospital with probability γ and then transitions to the recovered state. The exposed
 239 state node may die with the disease with probability of η . After transitioning to the recovered state and the
 240 dead state, the node is removed and does not participate in the propagation process in the crowd network.
 241 Considering node heterogeneity factors, the probability of a node being in each state at a time $(k + 1)$ is then
 242 given by Eqs. (5)-(9).

$$243 \quad P_i^S(k + 1) = S_i^S(k)(1 - \alpha_i), \quad (5)$$

$$244 \quad P_i^L(k + 1) = S_i^S(k)\alpha(i) + S_i^L(k)(1 - \beta), \quad (6)$$

$$245 \quad P_i^E(k + 1) = S_i^L(k)\beta + S_i^E(k)(1 - \gamma)(1 - \eta), \quad (7)$$

$$246 \quad P_i^R(k + 1) = S_i^E(k)(\gamma + 1), \quad (8)$$

$$247 \quad P_i^D(k + 1) = S_i^E(k)(\eta + 1), \quad (9)$$

248 where propagation probability $\alpha(i)$ represents the probability of node i spreading the virus. The exposed
 249 probability β is the proportion of nodes that change from the latent state to the exposed state per period. The
 250 recovered probability γ is the proportion of nodes that change from the exposed state to the recovered state in
 251 a period. The probability η of death is the proportion of nodes that change from the exposed state to the dead
 252 state per period. $\mathbf{S}_i(k + 1) = [S_i^S(k + 1), S_i^L(k + 1), S_i^E(k + 1), S_i^R(k + 1), S_i^D(k + 1)]$ is the state vector of
 253 the node i at the k -th period, where $S_i^S(k + 1), S_i^L(k + 1), S_i^E(k + 1), S_i^R(k + 1), S_i^D(k + 1) = 0, 1$, an

254 element equaling to 1 means that the node is at this state and an element equaling to 0 means that the node is
 255 not at this state. $S_i^S(k+1) + S_i^L(k+1) + S_i^E(k+1) + S_i^R(k+1) + S_i^D(k+1) = 1$ indicates that the node
 256 can only be at one of the five states in the k -th period.

257 $\mathbf{P}_i(k+1) = [P_i^S(k+1), P_i^L(k+1), P_i^E(k+1), P_i^R(k+1), P_i^D(k+1)]$ is the probability vector of
 258 node i at each state in the k -th period. These probabilities are normalized such that it indicates the probability
 259 of a node being at one of the five states, as shown in Eq. (10).

$$260 \quad P_i^S(k) + P_i^L(k) + P_i^E(k) + P_i^D(k) + P_i^R(k) = 1, \quad (10)$$

261 Time is divided into equal periods, and the state at any $(k+1)$ -th period is then given by:

$$262 \quad \mathbf{S}_i(k+1) = \text{MultiRealize}[\mathbf{P}_i(k+1)]. \quad (11)$$

263 where $\text{MultiRealize}[P_i(k+1)]$ is to randomly realize the state of node i in the k -th period according to the
 264 probability distribution of $\mathbf{P}_i(k+1)$.

265 **3. Cascading failure model of HIS's**

266 **3.1. Indicators of cascading failures of HIS's**

267 Let the hospitals in the city be regarded as nodes, denoted as H . The traffic roads between hospitals are
 268 connected by edges, denoted as L . The hospital infrastructure network is established, denoted as $U = G(H, L)$.

269 Suppose there are M hospital nodes and the adjacency matrix of U is $[M_{rs}]_{M \times M}$. $M_{rs} = 1$ if the hospital node
 270 r and the hospital node s have an edge ($r, s \in H$), $M_{rs} = 0$, otherwise.

271 The node of a hospital is responsible for patients in its catchment area, which is defined as the area where
 272 residents live in. The nearest neighbor classification method is used to classify individual nodes to hospital
 273 nodes in its proximity, as shown in Fig.2. The number of residents served by hospital node r is I_r . The patients
 274 with COVID-19 symptoms in the hospital catchment area will first choose that hospital for consultation, at
 275 this time, they enter 'HIS's as the load of the hospital node.

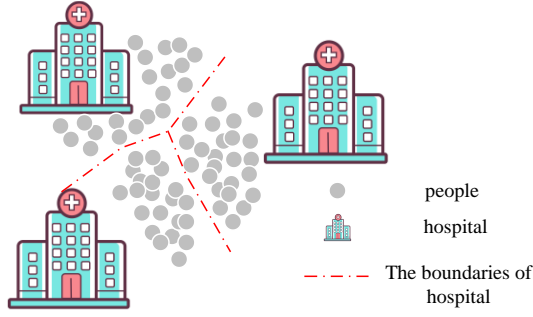


Fig. 2. The crowd in the hospital catchment area

276

277

278

279

280

281

282

283

284

285

286

287

288

289

290

291

292

293

294

295

The hospital admission rate is defined as the proportion of the population from the latent state to the exposed state in the population in the hospital catchment area per period, and it is denoted as φ_r . The hospital discharge rate is defined as the proportion of the population that transitions from an exposed state to a recovered state in the population in the hospital catchment area per period, and it is denoted as ω_r .

The outbreak rate $\mu_r(k)$ is an indicator of the hospital load and is defined as the ratio of the hospital admission rate to discharge rate:

$$\mu_r(k) = \frac{\varphi_r(k)}{\omega_r(k)}, \quad (12)$$

The threshold of the outbreak rate is 1. If $\mu_r(k) > 1$ then the hospital is said to be under attack. When the outbreak rate of a hospital node at one or more locations is larger than 1, the number of admissions is larger than the number of discharges and the total traffic flow of the hospital network rises, the corresponding hospital node is said to be under attack.

The basic regeneration number refers to the ability to quantify the transmission of an infectious disease and is a macroscopic concept that is widely used in infectious disease models. The basic regurgitation number depends on the outbreak rate of a hospital. The basic regurgitation number is directly proportional to the outbreak rate in hospitals. The outbreak rate is the ratio of hospital admissions to discharges per unit time, representing the average level of outbreaks over time, and this indicator already incorporates the effects of fluctuations in demand.

The state of a hospital is a comprehensive overall effect of the interaction of health staff and various types

296 of health care resources. A visual representation of the state of the hospital is the outbreak rate of the hospital.
 297 Under normal circumstances, hospital infrastructure is in equilibrium: the demand and supply of medical
 298 resources per unit of time are basically equal, the discharge rate is equal to the admission rate, and the outbreak
 299 rate is equal to 1. When the outbreak rate is greater than 1, the supply of medical resources per unit of time is
 300 insufficient, reflecting an active outbreak during this period.

301 The node load Q_r and node capacity C_r of the hospital are used to describe the workload of a node and
 302 working capacity in the process of network failures, respectively. The excess load $d_r(k)$ refers to the part of
 303 the node load exceeding the node capacity at the k -th period.

$$304 \quad d_r(k) = Q_r(k) - C_r, \quad (13)$$

305 where $Q_r(k)$ is the workload of hospital node r at the k -th period, C_r is the working capacity of hospital node
 306 r , $d_r(k)$ is the part of the node load exceeding the node capacity at the k -th period.

307 The resources such as medical staff and beds in a hospital needs to include the construction cost and the
 308 needs of the surrounding residents. Therefore, it is assumed that the node capacity is proportional to the number
 309 of catchment clusters of the hospital r (Albert, Jeong & Barabasi, 2001),

$$310 \quad C_r = I_r(1 + \rho_0), \quad (14)$$

311 where ρ_0 is an adjustable parameter that controls the capacity of the node, $\rho_0 \geq 0$, I_r is the number of elements
 312 in the set R_r , C_r is the capacity of hospital node r .

313 **3.2. Process analysis of cascading failures of HIS's**

314 Combined with the reality of the crowd's action in terms of proximity to a hospital, the first choice of all
 315 people at the initial moment is the nearest hospital for the treatment of COVID-19. The crowd moves along
 316 the traffic roads between hospitals, and the crowd has access to information about traffic conditions and
 317 hospitals, including the traffic flow on the roads, the remaining capacity of the hospital, and the road structure
 318 at a given moment. Under normal circumstances, the number of admissions and number of people discharged

319 per period are the same, and the total traffic volume of the entire hospital network per period is a fixed value.
320 When the outbreak rate of a hospital node at one or more locations exceeds a threshold, the number of
321 admissions exceeds the number of discharges and the total traffic flow of the hospital network rises, the
322 corresponding hospital node is said to be under attack. In this paper, interventions such as widespread
323 disinfection and epidemic prevention propaganda are not considered. The only actions occurring in the
324 population are daily activities, promptly seeking medical attention when symptoms are detected and choosing
325 a hospital.

326 In the process of cascading failures of hospital infrastructure networks, the hospital node has only normal
327 and failed states. The normal state means that the hospital still has free medical resources. The failed state
328 means that the hospital accepts too many patients and the node load Q_r exceeds node capacity C_r . By
329 comparing the node load and node capacity, the state of the hospital node can be judged. When the node load
330 exceeds the capacity of the node and the number of medical resources is in short supply, the node will fail.

331 Therefore, the specific process of node failures is as follows. When the outbreak rate of a node is greater
332 than 1, the number of newly increased patients in the hospital is more than that of cured patients, thus
333 generating a load increase. After the hospital receives the load increment, if the load of the node exceeds its
334 capacity, the node fails; otherwise, the node is in a normal state.

335 To reflect the actual supply and demand mechanism of the hospital, the load of the failed node is
336 distributed according to the actual situation. When the number of patients admitted by a hospital reaches its
337 saturation point, the hospital will continue to treat those patients that have already been admitted. The traffic
338 road connecting the hospital with other hospitals will not be abandoned. As the hospital does not have extra
339 beds, medical equipment or other resources, new patients cannot be admitted or treated there, and these patients
340 will go to other hospitals for treatment. Those patients who are receiving treatment in the hospital will continue
341 being treated. Therefore, the failed node is not removed, but acts as a transit node that no longer receives load.

342 The failed nodes can send out loads and can also be used as a transit node for other loads to move. Loads
 343 within the capacity of the node are received by the node and are no longer involved in the subsequent process.
 344 The load in excess of the node's capacity is seen as not being admitted to the hospital and needs to be
 345 redistributed.

346 Patients who have not been admitted by a hospital are more likely to choose the nearest hospital with
 347 more remaining capacity as the destination. Considering travel time and remaining capacity together, the
 348 attractiveness index of hospital s in case of node r failure is proposed as A_s^r . To maximize the benefit of
 349 moving the excess load to other normal nodes for treatment, the redistribution method considering the
 350 destination selection is carried out, as shown in Eqs. (15)-(17),

$$351 \quad A_s^r(k) = \frac{C_s - Q_s(k)}{T_{r \rightarrow s}}, \quad (15)$$

$$352 \quad \delta_{r \rightarrow s}(k) = \frac{A_s^r(k)}{\sum_{s \in H_1(k)} A_s^r(k)}, \quad (16)$$

353 and

$$354 \quad \sum_{s \in H_1(k)} \delta_{r \rightarrow s}(k) = 1, \quad (17)$$

355 where $A_s^r(k)$ is the index of attractiveness of node s to failed node r proposed in this paper, C_s is the capacity
 356 of hospital node s , $Q_s(k)$ is the load of hospital node r at the k -th period, $T_{r \rightarrow s}$ is the shortest travel time from
 357 failed node r to node s , $\delta_{r \rightarrow s}(k)$ is the ratio of the amount of load traveling from the failed node r to node s
 358 to the amount of excess load of node r , $H_1(k)$ is the set of normal hospital nodes at the k -th period.

359 All excess loads depart from the currently failed node and satisfy the starting traffic conservation
 360 condition.

$$361 \quad d_{r \rightarrow s}(k) = d_r(k) \delta_{r \rightarrow s}(k), \quad (18)$$

362 and

$$363 \quad \sum_{s \in H_1(k)} d_{r \rightarrow s}(k) = d_r(k), \quad (19)$$

364 where $d_r(k)$ represents the excess load that needs to be removed from the failed node r at the k -th period.

365 $d_{r \rightarrow s}(k)$ represents the excess load that needs to be moved from the failed node r to the node s at the k -th
 366 period.

367 After selecting the destination node for all the excess load, it is necessary to continue selecting the shortest
 368 path to the destination node to complete the flow distribution. The BPR impedance function is used to describe
 369 the crowding effect. Impedance is related to travel time and road congestion, as shown in Eq. (20).

$$370 \quad T_a(x_a) = T_a(0) \left(1 + \rho_1 \left(\frac{x_a}{C_a}\right)^{\rho_2}\right), \quad (20)$$

371 where $T_a(x_a)$ is the actual travel time of the selected route section a . $T_a(0)$ is the travel time when no one
 372 passes by on road section a . x_a is the excess load of the selected road section a , x is the set of excess loads for
 373 all sections, $x_a > 0$. C_a is the traffic capacity of section a . ρ_1 and ρ_2 are adjustable parameters.

374 Based on Eqs. (15) - (20) and the user balance distribution model, the distribution method is constructed,
 375 as shown in Eqs. (21)-(23),

$$376 \quad \min Z(x) = \min \sum_{a \in A} \int_0^{x_a} T_a(w) dw, \quad (21)$$

$$377 \quad \sum_{l \in L_{r \rightarrow s}} h_{r \rightarrow s}^l(k) = d_{r \rightarrow s}(k), \quad (22)$$

378 and

$$379 \quad x_a = \sum_{l \in L_{r \rightarrow s}} \sum_{r, s \in V} D_{r \rightarrow s}^{a, l}(k) h_{r \rightarrow s}^l(k), \quad (23)$$

380 where A is the set of road sections, and $T_a(w)$ is the impedance function on section a . Eq. (21) represents the
 381 shortest sum of travel time for all sections. $L_{r \rightarrow s}$ is the set of feasible routes between nodes r and s , l is one of
 382 the routes in $L_{r \rightarrow s}$, $h_{r \rightarrow s}^l(k)$ is the excess load of the l -th route between nodes r and s at the k -th period,
 383 $h_{r \rightarrow s}^l(k) \geq 0$, Eq. (22) indicates that the excess load from node r to s is the sum of the excess load of all
 384 possible routes. $D_{r \rightarrow s}^{a, l}(k)$ represents whether the l -th route between nodes r and s chooses road section a at the
 385 k -th period, if the l -th route contains road section a , then $D_{r \rightarrow s}^{a, l}(k) = 1$; otherwise, $D_{r \rightarrow s}^{a, l}(k) = 0$.

386 When the user balance distribution reaches its equilibrium, all the individuals in excess load will choose
 387 the route with the shortest travel time. There will be a situation where the travel time of all selected routes is

388 fixed, and the travel time of the selected route is less than that of all unselected routes. After the load is
389 redistributed, if the load of the new node exceeds the capacity, the node fails, and the cascading failure
390 continues occurring.

391 **3.3. Cascading failure model of HIS's**

392 The specific implementation phases of the cascading failure model of a HIS network are as follows.

393 Phase 1: At the initial moment, a small number of individuals are randomly selected to be set as patients
394 at the latent state and begin to spread the virus. The hospital infrastructure network is established. According
395 to the nearest neighbor classification method, the population is classified to different hospital nodes.

396 Phase 2: Determine the state of all patient nodes. Patients with an infected state enter their associated
397 hospital node in the catchment area according to the nearest neighbor classification. If there is no failure in the
398 corresponding hospital node, the patient load can enter the associated hospital smoothly. If the associated
399 hospital node has failed, the infected person is regarded as overloaded and enters phase 5.

400 Phase 3: Whether the hospital node outbreak rate exceeds the threshold or not is judged. When the
401 outbreak rate μ_r of one or more hospital nodes exceeds the threshold, the hospital nodes can be regarded as
402 being attacked. If the outbreak rate of all hospital nodes is lower than the threshold, no node will be attacked.

403 Phase 4: Determining whether a hospital node is failed under attacked or not. The corresponding hospital
404 node is attacked and the number of new patients entering the hospital network increases. The load increment
405 of the hospital network will go to the attacked hospital node r . When the load Q_r of the attacked hospital node
406 r is higher than its capacity C_r , the hospital node r is failed. The failed node is processed so that it no longer
407 receives load. The ability to transport loads is still retained, so that the loads within the capacity range are
408 absorbed, and the excess loads are redistributed. If the load of all nodes is less than the capacity, no failed
409 nodes will be generated.

410 Phase 5: Destination node selection and flow distribution for excess load. The user balance distribution

411 method considering destination selection is used to redistribute the excess load. Select a new hospital node
412 with a shorter arrival time and more remaining capacity as the destination for the excess load, and select the
413 shortest path to the new hospital node to complete the flow distribution.

414 Phase 6: Whether the failure is terminated is judged. If the load of all nodes after redistribution does not
415 exceed the node capacity, the failure is terminated. If there is a new node whose load is greater than the capacity
416 of the node after redistribution, a new failed node will be generated, the hospital network will be updated, and
417 phase 2 will be returned.

418 In the above six phases, phase 1 is executed at the initial moment, phase 2 - phase 6 are executed once in
419 each time period.

420 **4. Resilience optimization model for HIS's**

421 **4.1. Restoration of hospital**

422 The analysis in this section is only for failed nodes. Node restoration is defined as the process of bringing
423 a failed node back to a normal state. If the failed node is restored only by increasing the node capacity, the
424 failed node can certainly continue to receive more patients in a short period, and the performance of the node
425 will be improved in a short period. However, its outbreak rate remains unacceptably high, with far more new
426 hospital admissions than new hospital discharges per period. The node load will inevitably exceed the node
427 capacity again within a limited time. Therefore, in order to restore failed nodes, restoration measures to reduce
428 the outbreak rate and increase node capacity should be implemented at the same time. The specific measures
429 are as follows.

430 1) Improving the hospital discharge rate ω_r by increasing the production of medical resources such as
431 personal protective equipment (PPE) and disinfectants. This type of medical resources will be consumed in a
432 short period and needs to be supplied to hospitals at a high frequency. By increasing the inventory of such
433 resources of the failed node, the outbreak rate can be reduced. The failed node can be gradually restored to a

434 normal state.

435 2) Increasing the node capacity of a hospital by requisitioning hotels near the hospital and establishing
436 temporary hospitals. As the capacity of the node increases, the node can accommodate more patients, thereby
437 reducing the number of loads transferred out of the node. The capacity that can be added to each hospital node
438 is a finite fixed value.

439 Only one node can be restored within a period, and other nodes will not take any measures. After a node
440 has been performed multiple restoration measures, the outbreak rate gradually decreases until it drops below
441 1, and the node is gradually restored to a normal state.

442 **4.2. The restoration benefits of hospital**

443 When the outbreak rate of hospital node r is greater than 1, the number of new hospital admissions is
444 greater than that of new hospital discharges per period. The difference between the number of new hospital
445 admissions and the number of new hospital discharges is the restoration demand of hospital node r . The
446 restoration demand of hospital node r is denoted as $\Delta D_r(k)$, which can account for the net increase of patients
447 in a hospital node per period, as shown in Eq. (24).

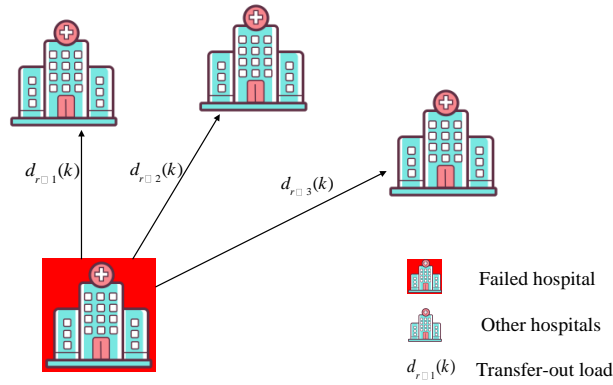
$$448 \quad \Delta D_r(k) = (\varphi_r(k) - \omega_r(k))N_r, \quad (24)$$

449 where N_r represents the number of residents in the catchment area of the hospital node r , $\varphi_r(k)$ is the
450 hospital admission rate of node r at the k -th period, $\omega_r(k)$ is the hospital discharge rate of node r at the k -th
451 period.

452 Between phases 4 and 5 of cascading failure model in Section 3.3, restoration actions are to be executed
453 on the failed node, i.e., increase the hospital node capacity. There are 3 cases after performing the restoration
454 actions, as shown below.

455 (1) Action effect 1. Non-executing measures were implemented on the failed hospital nodes. All the excess
456 loads are transferred to other normal hospitals. The transfer-out load of node r is $\Delta D_r(k) = \sum_{s \in H_1} d_{r \rightarrow s}(k)$.

457 $\sum_{s \in H_1} d_{r \rightarrow s}(k)$ represents the excess load transferred from the node r to the normal nodes at the k -th period.

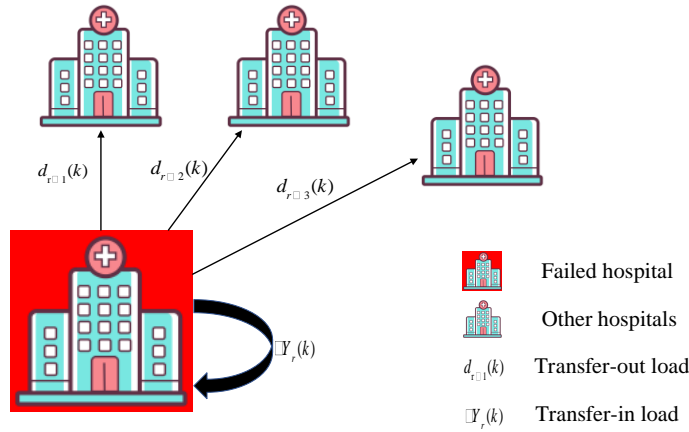


458

459 Fig. 3. Action effect 1

460 (2) Action effect 2. After performing restoration measures on the failed node, the node has a transfer-out

461 load and a transfer-in load.



462

463 Fig. 4. Action effect 2

464 After performing restoration measures on the failed node, the capacity of the failed hospital increased by

465 $\Delta C_r(k)$. The newly added capacity $\Delta C_r(k)$ is less than $\Delta D_r(k)$, the loads d_{ri} that cannot be accommodated by

466 node r is used as the transfer-out load to hospital node i . In this case, $\Delta Y_r(k)$ is the transfer-in load and

467 $\Delta Y_r(k) = \Delta C_r(k)$. $\sum_{s \in H_1} d_{r \rightarrow s}(k)$ represents the excess load transferred from the node r to the normal node s

468 at the k -th period, $\sum_{s \in H_1} d_{r \rightarrow s}(k) + \Delta Y_r(k) = \Delta D_r(k)$.

469 (3) Action effect 3. After performing restoration measures on the failed node, the node only has a transfer-

470 in load.

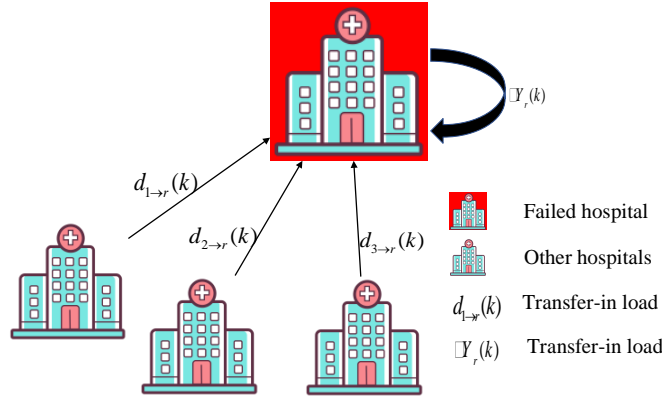


Fig. 5. Action effect 3

471

472

473 After performing restoration measures on the failed node, the capacity of the failed node increases. The
 474 newly added capacity $\Delta D_r(k)$ is able to accommodate the full restoration demand and there may be spare
 475 capacity that can be used to accommodate the load $d_{s \rightarrow r}$ that people transferred from other failed nodes. In
 476 this case, $\sum_{s \in H_2} d_{s \rightarrow r}(k) + \Delta Y_r(k) = \Delta C_r(k)$, and $\Delta Y_r(k) = \Delta D_r(k)$. $\Delta Y_r(k)$ are the amount of transfer-in
 477 load of hospital node r from itself, $\sum_{s \in H_2} d_{s \rightarrow r}(k)$ represents the excess load transferred from the failed node
 478 s to node r at the k -th period.

479 A node transfers patients to other nodes, indicating that the node is not capable of receiving all patients
 480 within its catchment area and can be considered a loss of performance for that node. If the node is able to meet
 481 the access needs of all patients within its catchment area, or even accept patients from other nodes, this can be
 482 considered as an increase in performance for that node. Therefore, the loss of performance of a node can be
 483 expressed in terms of transfer-out load. The more transfer-out load, the more performance loss. The increase
 484 in the performance of a node can be expressed in terms of transfer-in load. The more transfer-in load, the more
 485 performance increase.

486 Resilience theory is used to describe the ability of nodes to cope with emergencies, as well as to quantify
 487 the cumulative effect of restoration measures on node performance recovery over previous periods.

488 In this paper, the hospital node resilience is defined as the ratio of the cumulative performance gain to the
 489 performance loss of a node at the k -th period. The greater the ratio, the greater the resilience of the node. The

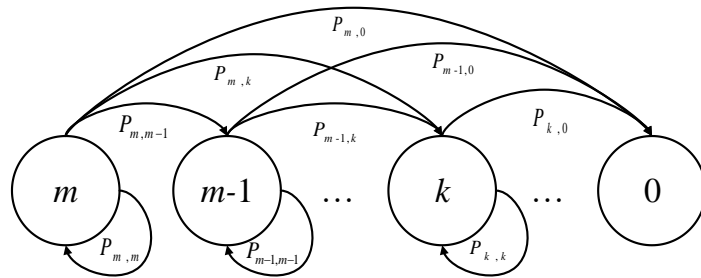
490 resilience of hospital node r at the k -th period is calculated as shown in Eq. (25).

491
$$g^r(k) = \sum_{p=0}^k \frac{\Delta Y_r(p) + \sum_{s \in H_2} d_{s \rightarrow r}(p)}{\sum_{s \in H_1} d_{r \rightarrow s}(p)}, \quad (25)$$

492 where k is an integer, and $k > 0$, $g^r(k)$ denotes the resilience of hospital node r at the k -th period.
 493 $\Delta Y_r(p)$ represents the transfer-in load from itself at the p -th period, p is an integer, $p > 0$. $\sum_{s \in H_2} d_{s \rightarrow r}(p)$
 494 represents the excess load transferred from the failed node s to node r at the p -th period.
 495 $\sum_{s \in H_1} d_{r \rightarrow s}(p)$ represents the excess load transferred from the node r to the normal node s at the p -th period.
 496 From equation (25), we can see that hospital resilience $g^r(k)$ increases with $\Delta Y_r(p)$, $\sum_{s \in H_2} d_{s \rightarrow r}(p)$, and
 497 decreases with $\sum_{s \in H_1} d_{r \rightarrow s}(p)$. The capacity and speed of access to a hospital can affect all these three
 498 indicators, resilience as an inherent property of hospitals, can be improved by implementing two kinds of
 499 restoration measures in Section 4.1.

500 **4.3. Resilience optimization of HIS's based on Markov decision process**

501 In the restoration process, the states of the nodes are not merely normal and failed, the restoration process
 502 with gradually decreasing outbreak rate can be discretized into multiple states with different outbreak rates
 503 (Zeng, Fang, Zhai & Du ,2021) Let $S(k)$ be the state of the node at the k -th period, which is used to reflect the
 504 restoration degree of the hospital, $S(k) \in S = \{0,1,2, \dots, m\}$. The larger the value, the larger the outbreak rate
 505 of the node. $S(k) = m$ corresponds to the level of outbreak rate when the node fails, $S(k) = 0$ means the node
 506 is in a normal state, corresponding to the level of node outbreak rate less than or equal to 1. The process of
 507 node state transition during the restoration process is shown in Fig. 6.



508
 509 Fig. 6. the process of node state transfer during the restoration process

510 In order to optimize the resilience of hospital nodes, the Markov decision process (MDP) approach is

511 used. The MDP is of the form of a quadruplet: $\{S, (B(i), i \in S), P, R\}$. (See [Supporting Information](#) for details
 512 [on modeling the Markov decision process](#)).

513 $R(k) = \{r(i, b), b \in B(i), i \in S\}$, $r(i, b)$ is the reward function, $R(k)$ denotes the expected reward
 514 received by the node when is in state i at the k -th period and takes action b . In this paper, $R(k)$ is defined as
 515 the sum of the resilience of all nodes at the k -th period, and the formula is as shown in Eq. (26),

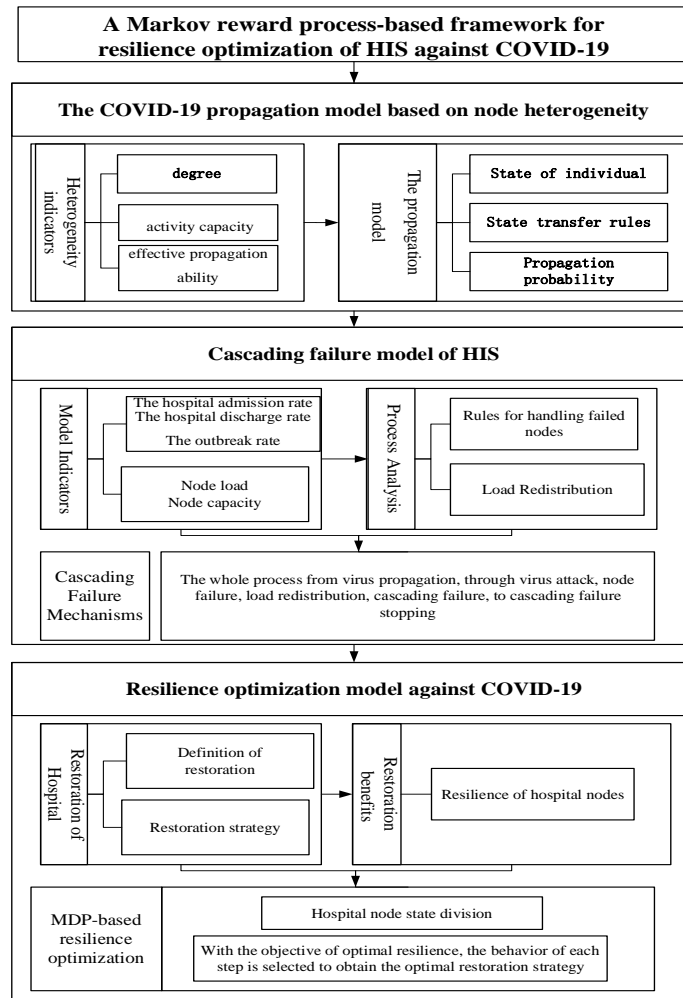
$$516 \quad R(k) = \sum_{r \in H} g^r(k) = \sum_{r \in H} \sum_{p=0}^k \frac{\Delta Y_r(p) + \sum_{s \in H_2} d_{s \rightarrow r}(p)}{\sum_{s \in H_1} d_{r \rightarrow s}(p)} \quad (26)$$

517 With the objective of maximizing the sum of the resilience of all nodes, the node restoration strategy is
 518 found for each moment, as in Eq. (27),

$$519 \quad \max R(k) = \sum_{r \in H} g^r(k) = \sum_{r \in H} \sum_{p=0}^k \frac{\Delta Y_r(p) + \sum_{s \in H_2} d_{s \rightarrow r}(p)}{\sum_{s \in H_1} d_{r \rightarrow s}(p)}, \quad (27)$$

520 where k is an integer, and $k > 0$, $g^r(k)$ denotes the resilience of hospital node r at the k -th period.
 521 $\Delta Y_r(p)$ represents the transfer-in load from itself at the p -th period. p is an integer, $p > 0$. $\sum_{s \in H_2} d_{s \rightarrow r}(p)$
 522 represents the excess load transferred from the failed node s to node r at the p -th period.
 523 $\sum_{s \in H_1} d_{r \rightarrow s}(p)$ represents the excess load transferred from the node r to the normal node s at the p -th period,
 524 H represents the set of all the hospital nodes, $R(k)$ is the resilience of HIS's, which is also the reward function
 525 of HIS's.

526 Based on the COVID-19 propagation model, the cascading failure model and the resilience optimization
 527 model, we can obtain the Markov reward process-based framework for resilience optimization of HIS's against
 528 COVID-19, as shown in Fig. 7.



529

530 Fig. 7. the Markov reward process-based framework for resilience optimization of HIS's against COVID-19

531 **5. Application**

532 **5.1. Data and methods of simulation**

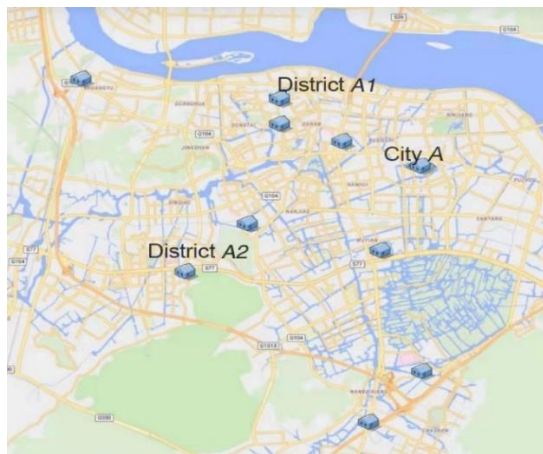
533 Real data from Lucheng District and Ouhai District of Wenzhou City, Zhejiang Province, China, are used
 534 as examples for simulation. To avoid disclosing national security information, we name Wenzhou city as City A,
 535 Lucheng district as district A, and Ouhai district as District B. There are two districts, A1 and A2, in City A,
 536 for example. There are six hospitals in District A1 and four in District A2, with the number of hospital beds
 537 shown in Table 1S (shown in Supporting Information).

538 For the research, the population data of each street in City A was used to reflect the reality of the
 539 population distribution. The administrative centers of street settlements were used as a proxy for the center of
 540 gravity of the population. 14 street townships are within the area of District A1, and 13 street townships are

541 within the area of District A2, as shown in Table 2S (shown in Supporting Information), with data from the
542 2019 Statistical Yearbook of the Bureau of Statistics of City A.

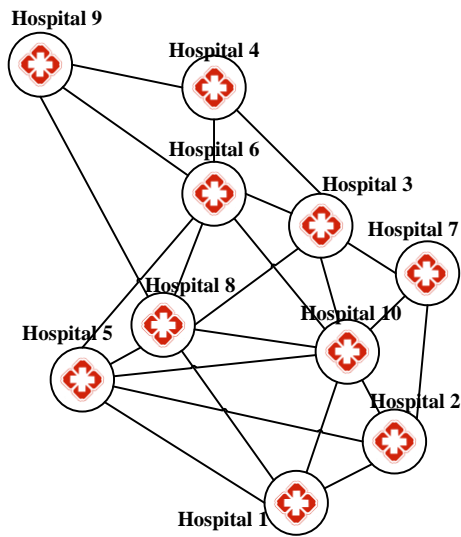
543 After collecting the data, an agent-based simulation model is built using a software package entitled
544 *Anylogic* to realize the crowd virus propagation and hospital node cascading failure process. Pathmind, which
545 is a SaaS platform that enables businesses to apply reinforcement learning to real-world scenarios without data
546 science expertise, was integrated to enable MDP driven node resilience optimization. The simulation process
547 is as follows.

548 Step 1: Constructing a hospital infrastructure network for Districts A1 and A2 in city A, as shown in Fig.
549 8. The blue building icons in the GIS map represents hospitals, which are connected to each other by roads.



550
551 Fig. 8. Map of Districts A1 and A2, city A

552 A network of hospital infrastructure in Districts A1 and A2 in City A is created, using the hospitals as
553 nodes and connecting roads as edges, as shown in Fig. 9.



554

555

Fig.9.Hospital infrastructure network in Districts A1 and A2

556

Step 2: Refinement of the agent. To achieve the virus propagation and cascading failure process under the

557

COVID-19 outbreak, the internal attributes and functions of community and hospital agents are set. As shown

558

in Fig. 10, the left community agent has different area names, area population and contains people agent, which

559

represents the residential population. The right hospital agent has two attributes of node names and node

560

capacity. Four variables are set for the hospital agent: the number of current patients, whether it is in a failed

561

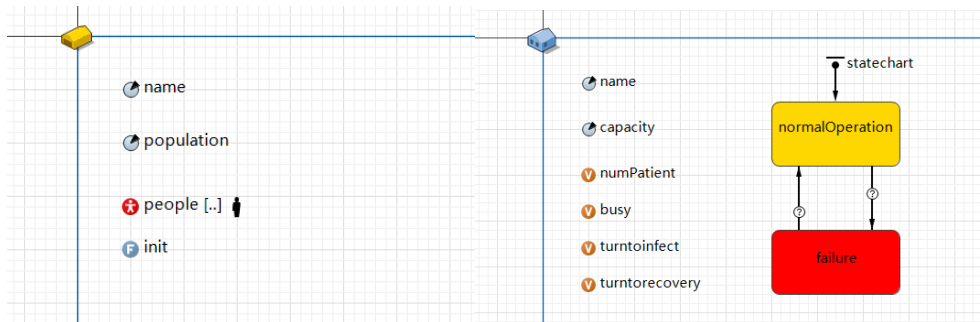
state or not, the hospital admission rate and hospital discharge rate that are set to record the operation of each

562

node. The node load is represented by the current number of patients and is used to determine whether or not

563

the node status is failed in the state diagram on the right.



564

565

Fig.10. Community agent (left) and Hospital agent (right)

566

As shown in Fig. 11, for each person within the community agent, the number of daily contacts, action

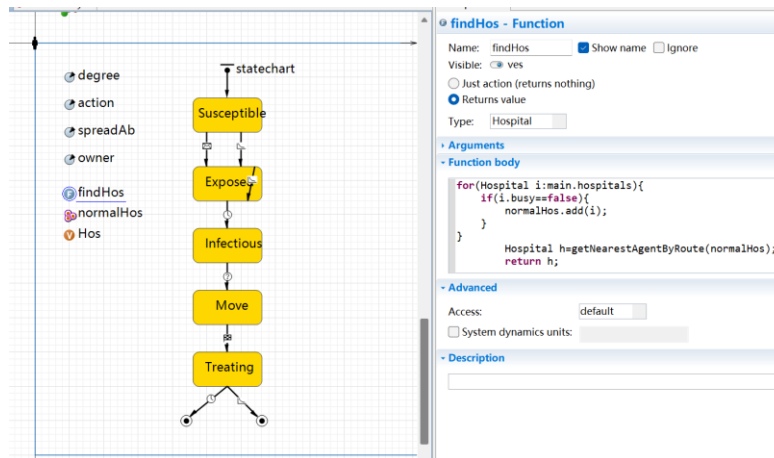
567

capacity and spread capacity differ, as shown by the parameters in the Fig. 11. The yellow state diagram on the

568

right indicates the spread of the virus within the population. After going through the susceptible, latent and

569 infectious states, individuals in the infectious state will call the function *findHos* to find the nearest hospital
 570 node that has not failed and will travel along the traffic path. Based on the proposed load allocation model as
 571 shown in Eqs. (21)-(23), the function *findHos* in this paper is defined to allocate traffic for failed hospital nodes.
 572 The infectious individual reaches the node and begins treatment, and then enters the death state with certain
 573 probability, or the cure state with a delay.



574
 575 Fig. 11. People agent within Community agent

576 The cascading failure process is mainly reflected by the function *findHos*. When the *findHos* function is
 577 called by an infectious individual, all hospital nodes are stored in the set *normalHos* in Fig. 11 and the nearest
 578 node is found in the set. If the nearest hospital node enters a failed state, it is removed from the set and the
 579 search for the most suitable node in the set is continued with the objective of being the closest and smallest.
 580 Consideration of traffic impedance along the route is omitted here. After finding the most suitable node, calling
 581 all of the functions is completed, the infectious individual travels to the most suitable node.

582 Step 3: Outputting node attribute value data during cascading failures and integrate *Pathmind* for
 583 resilience optimization. Four metrics including the admission rate, the discharge rate, the node load, and
 584 whether the node is disabled, are recorded and output for each period of the hospital node. The data is randomly
 585 taken at the 15-th, 35-th and 55-th periods, respectively. The nodes were divided into six states based on the
 586 outbreak rate of nodes in different ranges, as shown in Table 3S (shown in Supporting Information).

587 Assign value to the probability $P(j|i, b)$ of transferring to state j after doing act b in state i , please see

588 **Supporting Information.**

589 Using the Pathmind Helper to introduce MDP into Anylogic. Pathmind Helper is an AnyLogic palette
590 item. Drop Pathmind Helper into the model and use it to add MDP functions. Starting from the selected moment,
591 the current state of the node, the outbreak rate is observed and the node is made to behave. Let only one node
592 be restored at a period, and calculate the marginal benefit of making the action at each moment.

593 Step 4: Uploading the simulation model to the Pathmind cloud. Train the model with the objective of
594 maximizing the resilience of all nodes to obtain the best action strategy. Download the strategy trained by
595 Pathmind and verify the optimum in Anylogic.

596 **5.2. Analysis of simulation results**

597 The results of the cascading failure are shown in Figs.12, 13, and 14, respectively, in which the black
598 character icon represents the infectious individuals, the black character icon walking on the road indicates that
599 the infectious individuals have left their places of residence to go to the hospital to seek treatment. The red
600 building icons represent failed hospital nodes, the blue ones represent normal hospital nodes, and the yellow
601 ones represent population residences. The number of failed hospital nodes increases with time, from 2 at the
602 15-th period to 3 at the 35-th period and finally to 5 at the 55-th period, causing the cascading failure effect.



Fig. 12. Cascading failure results at the 15-th period Fig. 13. Cascading failure results at the 35-th period Fig. 14. Cascading failure results at the 55-th period

603 As can be seen in Figures 12-14, if restoration actions are not implemented, an HIS will suffer from
604 serious cascading failures. Therefore, it is necessary to implement restoration actions for the HIS in time. Take

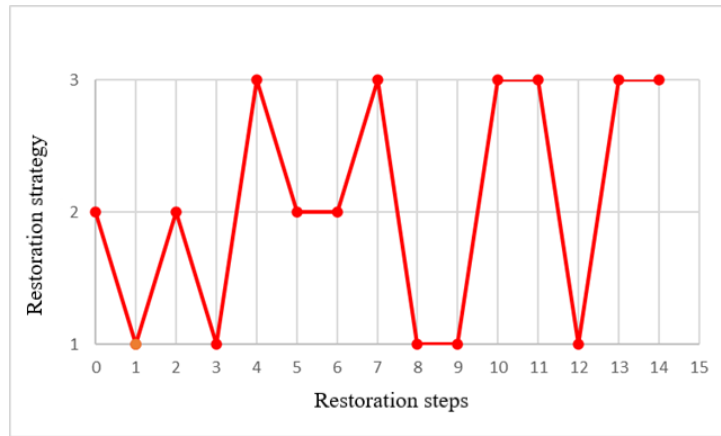
605 the cascading failure case at the 35-th period as an example and calculate the optimal restoration strategy for
606 resilience. The failed nodes at the 35-th period are hospitals 5, 9 and 10, respectively. All three nodes, which
607 are in state 5, have an outbreak rate greater than 1.2. With the objective of maximizing the sum of the resilience
608 of all nodes, based on the MDP, the restoration strategy is obtained, as shown in Table 1. The actions are [1, 0,
609 0], [0, 1, 0] and [0, 0, 1], respectively, representing the restoration measures performed on hospitals 5, 9 and
610 10 in the current step, respectively. Which node we should repair at each step? The question is addressed by
611 the restoration strategy in Table 1. Only one failed node is repaired at each step and the node state changes at
612 the next step. Since the change of the hospital state is a stochastic process, a total of 15 steps of restoration
613 strategy are taken to restore all three failed nodes to normal state 0. From Table 1, the nodes 9, 5, 9, 5, 10, 9,
614 9, 10, 5, 5, 10, 10, 5, 10, and 10 are repaired at steps 0-14, respectively.

Table 1. The MDP-based restoration strategies for optimal resilience at the 35-th period

Step	State of the Hospital 5	State of the Hospital 9	State of the Hospital 10	Strategy (effective at the next step)
0	5	5	5	[0,1,0]
1	5	3	5	[1,0,0]
2	4	3	5	[0,1,0]
3	4	2	5	[1,0,0]
4	2	2	5	[0,0,1]
5	2	2	4	[0,1,0]
6	2	1	4	[0,1,0]
7	2	0	4	[0,0,1]
8	2	0	3	[1,0,0]
9	2	0	3	[1,0,0]
10	1	0	3	[0,0,1]
11	1	0	2	[0,0,1]
12	1	0	2	[1,0,0]

13	0	0	2	[0,0,1]
14	0	0	1	[0,0,1]
15	0	0	0	

615 The line graph shown in Fig. 15 provides a visual illustration of the restoration measures for the 35th
616 period, with actions 1, 2 and 3 representing the execution of restoration strategies for hospitals 5, 9 and 10,
617 respectively, in the current step.



618
619 Fig. 15. MDP-based resilience optimization restoration strategy at the 35-th period

620 The restoration effect after applying the optimal action strategy is shown in Figs. 16, 17 and 18,
621 respectively. The red buildings in the figure represent failed nodes, the green ones represent nodes that have
622 been restored to a normal state and the blue ones represent normal nodes that have never failed. It can be seen
623 that hospital 9 is restored to normal, then hospital 5 is restored to normal, and finally hospital 10 is restored to
624 normal.

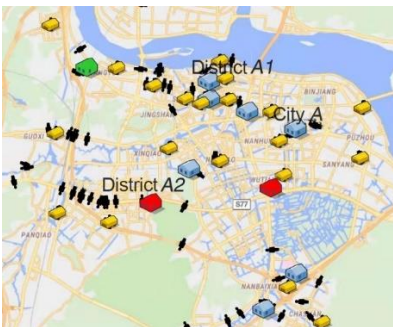


Fig. 16. Hospital 9 returns to normal

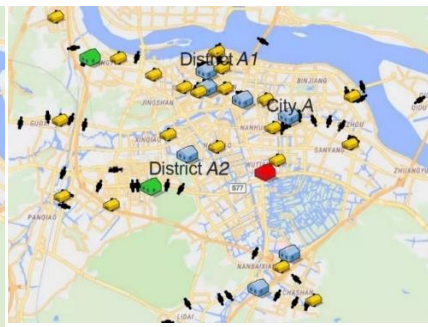


Fig. 17. Hospital 5 returns to normal

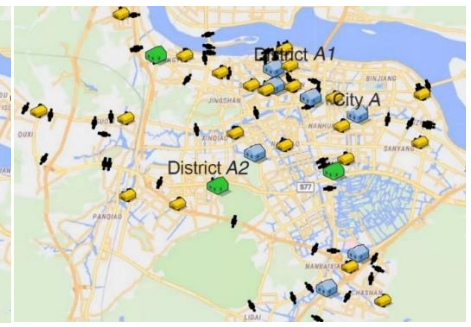
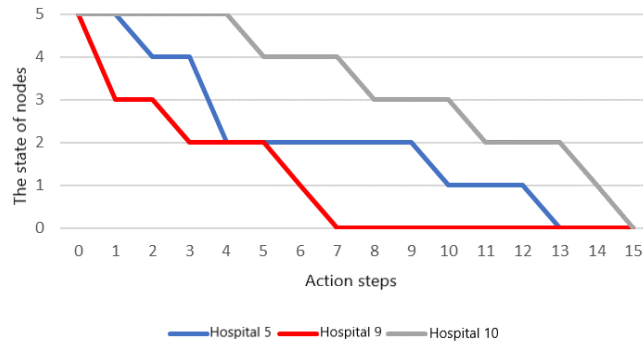


Fig. 18. Hospital 10 returns to normal

625 After applying the optimal action strategy, a graph illustrating the changes between node states during the
626 MDP-based resilience optimal restoration process is shown in Fig. 19.



627
628 Fig. 19. State changes of nodes during MDP-based resilience optimal restoration process

629 From Fig. 19, we can see the state change of the three failed nodes in the 35-th period. We can see that
630 node 9 is the first to return to its normal state, node 5 is the second to return to its normal state, and node 10 is
631 the last to return to its normal state.

632 6. Conclusions and future work

633 6.1. Research content

634 This paper used the Markov decision process to analyze the resilience of HIS under the attack of the
635 COVID-19. First, a COVID-19 propagation model based on node heterogeneity was developed, and a
636 cascading failure model for HIS's based on the virus propagation model was developed. Then, based on the
637 virus propagation model and the cascading failure model, a resilience optimization model for HIS's was
638 established, which provides a framework for restoration of hospital infrastructure in response to public health
639 emergencies. Finally, this paper illustrated the applicability of the model proposed in this paper with a real
640 case, which is beneficial for readers to clearly understand the performance change of HIS before and after the
641 occurrence of an emergency event and how to develop a remediation strategy.

642 6.2. Managerial implication

643 The results of this paper can provide a useful reference to people in the emergency management of HIS.
644 First, if the failed node is not repaired in time, the HIS undergoes cascading failures. Therefore, hospital

645 managers should assess the states of their HIS's in time and take timely measures such as increasing beds and
646 speeding up access for medical treatment to reduce losses.

647 Second, managers should focus on the state of the hospital. A hospital is a single node of HIS on the one
648 hand, and a system of staffs, patients and various medical resources interacting with each other on the other
649 hand. There are many indicators to evaluate the state of a HIS from different perspectives. In this paper, we
650 proposed the concept of the outbreak rate to evaluate the hospital states from the patients' perspective, which
651 can measure the attacks on the HIS's over a period of time. Therefore, hospital managers should not only
652 consider the number of admitted patients, but also the number of discharged patients. In addition, three
653 scenarios of hospitals after maintenance were discussed to provide a basis for managers to evaluate the actual
654 status of HIS's.

655 Third, managers of a HIS should focus on the performance of the hospital infrastructure network when
656 making decisions on restoration. When making maintenance decisions, there are many optimization objectives.
657 Resilience, as an indicator of a system's ability to withstand external risks, can reduce the risks associated with
658 the inevitable disruption of systems. Determining the restoration measures based on the resilience optimization
659 model can ensure the maximum resilience of the HIS, i.e., the maximum capacity of the HIS to serve patients
660 after a disaster. Therefore, managers of HIS's can manage risk with the goal of optimizing the resilience of the
661 entire system.

662 **6.3. Future work**

663 The study of the propagation characteristics of COVID-19 in this paper did not consider realistic factors
664 such as isolation interventions and information dissemination or the multiple failed states of nodes during
665 cascading failures. Those limitations will be studied in the future. Based on the study, further research can be
666 conducted on the following concerns:

667 (1) Introduce isolation interventions into the virus transmission model in the study.

668

669 (2) Consider the state of the hospital as a continuous variable in the study of hospital resilience.

670 (3) Introduce importance measures in the study to determine the maintenance priority of different
671 hospitals.

672 (4) Study the impact of different types of maintenance measures on hospital resilience.

673 **References**

674 Achour, N., Miyajima, M., Pascale, F., & Price, A. D. F. (2014). Hospital resilience to natural hazards:
675 classification and performance of utilities. *Disaster Prevention & Management*, 23(1):40-52.

676 <https://doi.org/10.1108/DPM-03-2013-0057>.

677 Albert, R., Jeong, H., & Barabasi, A. L. (2001). Erratum: correction: Error and attack tolerance of complex
678 networks. *Nature*, 409(6819): 542-542. <https://doi.org/10.1038/35054111>.

679 Almoghathawi, Y. & Barker, K. (2019). Component importance measures for interdependent infrastructure
680 network resilience. *Computers & Industrial Engineering*, 133,153-164.

681 <https://doi.org/10.1016/j.cie.2019.05.001>.

682 Barabadi, A., Ghiasi, M. H., & Nouri, A. (2020). Qarahasanlou A N. A Holistic View of Health Infrastructure
683 Resilience before and after COVID-19. *Archives of Bone and Joint Surgery*, 8:262-269.

684 <https://doi.org/10.22038/abjs.2020.47817.2360>.

685 Barasa, E. W., Mbau, R. & Gilson, L. (2018). What is resilience and how can it be nurtured? a systematic
686 review of empirical literature on organizational resilience. *International Journal of Health Policy &*

687 *Management*, 7(6). <https://doi.org/10.15171/ijhpm.2018.06>.

688 Broek, M., Teunter, R., Jonge, B. D., & Veldman, J. (2019). Joint condition-based maintenance and condition-
689 based production optimization, *Reliability Engineering and System Safety*, 214: 107743.

690 <https://doi.org/10.1016/j.ress.2021.107743>.

691 Broek, M., Teunter, R. H., Jonge, B. D. & Veldman, J. (2021). Joint condition-based maintenance and load-
692 sharing optimization for two-unit systems with economic dependency - sciencedirect. *European Journal*
693 *of Operational Research*, 295(3): 1119-1131. <https://doi.org/10.1016/j.ejor.2021.03.044>.

694 Enatsu, Y., Messina, E., Nakata, Y., Muroya, Y. & Vecchio, R. A. (2012). Global dynamics of a delayed sirs
695 epidemic model with a wide class of nonlinear incidence rates. *Journal of Applied*
696 *Mathematics&Computing*, 39: 15-34. <https://doi.org/10.1007/s12190-011-0507-y>.

697 Gagliardi, H. F. & Alves, D. (2010). Small-world effect in epidemics using cellular automata. *Mathematical*
698 *Population Studies*, 17(2): 79-90. <https://doi.org/10.1080/08898481003689486>.

699 [Galaitis, S. E., Keisler, Jeffrey M., Trump, Benjamin D. & Linkov, Igor. \(2020\). The need to reconcile concepts](#)
700 [that characterize systems facing threats. *Risk Analysis*, 41\(1\): 3-15. <https://doi.org/10.1111/risa.13577>.](#)

701 Gao, S. & Wang, H. (2022). Scenario prediction of public health emergencies using infectious disease
702 dynamics model and dynamic Bayes. *Future Generation Computer Systems*, 127: 334-346.
703 <https://doi.org/10.1016/j.future.2021.09.028>.

704 Grimaz, S., Ruzzene, E. & Zorzini, F. (2021). Situational assessment of hospital facilities for modernization
705 purposes and resilience improvement, *International Journal of Disaster Risk Reduction*, 66: 102594.
706 <https://doi.org/10.1016/j.ijdr.2021.102594>.

707 Guo, N., Guo, P., Dong, H. Y., Zhao, J. & Han, Q. Y. (2019). Modeling and analysis of cascading failures in
708 projects: A complex network approach. *Computer & Industrial Engineering*, 127: (1-7).
709 <https://doi.org/10.1016/j.cie.2018.11.051>.

710 Hassan, E. M. & Mahmoud, H. N. (2021), Orchestrating performance of healthcare networks subjected to the
711 compound events of natural disasters and pandemic. *Nature Communications*, 12(1): 1338,
712 <https://doi.org/10.1038/s41467-021-21581-x>.

713 Hosseini, S., Barker, K. & Ramirez-Marquez, J. E. (2016). A review of definitions and measures of system

714 resilience. *Reliability Engineering and System Safety*, 145: 47-61.
715 <https://doi.org/10.1016/j.ress.2015.08.006>.

716 Hynes, W., Trump, B.D., Love, P & Linkov, I. (2020). Bouncing forward: A Resilience Approach to dealing
717 with COVID-19 and future systemic shocks. *Environment, Systems, Decisions*, 40(2): 174-184.
718 <https://doi.org/10.1007/s10669-020-09776-x>.

719 Keizer, M., Teunter, R. H. & Veldman, J. (2017). Joint condition-based maintenance and inventory
720 optimization for systems with multiple components. *European Journal of Operational Research*. 257(1):
721 209-222. <https://doi.org/10.1016/j.ejor.2016.07.047>.

722 Kermack, W. O. & Mckendrick, A. G. (1991). A contribution to the mathematical theory of epidemics. *Bulletin*
723 *of Mathematical Biology*, 53(1-2): 57-87. [https://doi.org/10.1016/S0092-8240\(05\)80042-4](https://doi.org/10.1016/S0092-8240(05)80042-4).

724 Li, X., Guo, J., Gao, C., Zhang, L.Y. & Zhang, Z. L. (2018). A hybrid strategy for network immunization.
725 *Chaos Solitons & Fractals*, 106:214-219. <https://doi.org/10.1016/j.chaos.2017.11.029>.

726 Li, Z., Li, N., Cimellaro, G. P. & Fang, D. (2020). System Dynamics Modeling-Based Approach for Assessing
727 Seismic Resilience of Hospitals: Methodology and a Case in China. *Journal of Management in*
728 *Engineering*, 36(5): 04020050. [https://doi.org/10.1061/\(ASCE\)ME.1943-5479.0000814](https://doi.org/10.1061/(ASCE)ME.1943-5479.0000814).

729 Linkov, I., Fox-Lent, C., Read, L., Allen, C. R., Arnott, J. C., Bellini, E., Coaffee, J., Florin, M. V., Hatfield,
730 K. & Hyde, I. (2018). Tiered Approach to Resilience Assessment, *Risk Analysis*, 38(9): 1772-1780.
731 <https://doi.org/10.1111/risa.12991>.

732 Linkov, I., Keenan, J. M. & Trump, B. D. (2021). COVID-19: systemic risk and resilience. Springer,
733 Amsterdam, The Netherlands. <https://doi.org/10.1007/978-3-030-71587-8>.

734 Ouyang M. (2017). A mathematical framework to optimize resilience of interdependent critical infrastructure
735 systems under spatially localized attacks. *European Journal of Operational Research*, 262(3):
736 <https://doi.org/10.1016/j.ejor.2017.04.022>

- 737 Pishnamazzadeh, M., Sepehri, M. M. & Ostadi B. (2020). An Assessment Model for Hospital Resilience
738 according to the Simultaneous Consideration of Key Performance Indicators: A System Dynamics
739 Approach. *Perioperative Care and Operating Room Management*, 20.
740 <https://doi.org/10.1016/j.pcorn.2020.100118>.
- 741 Qian, X., & Ukkusuri, S. V. (2021). Connecting urban transportation systems with the spread of infectious
742 diseases: a trans-seir modeling approach. *Transportation Research Part B Methodological*, 145(3): 185-
743 211. <https://doi.org/10.1016/j.trb.2021.01.008>.
- 744 Ransolin, N., Saurin, T. A. & Formoso, C. T. (2020). Integrated modelling of built environment and functional
745 requirements: implications for resilience. *Applied Ergonomics*, 88: 103154.
746 <https://doi.org/10.1016/j.apergo.2020.103154>.
- 747 Rodríguez-Méndez, V. Ser-Giacomi, E. & HernándezGarcía E. (2017). Clustering coefficient and periodic
748 orbits in flow networks. *Chaos*, 27(3). <https://doi.org/10.1063/1.4971787>.
- 749 Samsuddin, N. M., Takim, R., Nawawi, A. H., & Alwee, S. N. A. S. (2018). Disaster Preparedness Attributes
750 and Hospital's Resilience in Malaysia. *Procedia Engineering*, 212:371-378.
751 <https://doi.org/10.1016/j.proeng.2018.01.048>.
- 752 Sekiguchi, M. & Ishiwata, E. (2010). Global dynamics of a discretized sirs epidemic model with time delay.
753 *Journal of Mathematical Analysis & Applications*, 371(1), 195-202.
754 <https://doi.org/10.1016/j.jmaa.2010.05.007>.
- 755 Sheu, S.-H., Liu, T.-H., Zhang, Z.-G., & Tsai, H.-N. (2020). Optimum replacement policy for cumulative
756 damage models based on multi-attributes. *Computers & Industrial Engineering*, 139, 106206.
757 <https://doi.org/10.1016/j.cie.2019.106206>.
- 758 Siskos, E. & Burgherr, P. (2022). Multicriteria Decision Support for the Evaluation of Electricity Supply
759 Resilience: Exploration of Interacting Criteria. *European Journal of Operational Research*, 298(2): 611-

760 626. <https://doi.org/10.1016/j.ejor.2021.07.026>.

761 Tariverdi, M., Fotouhi, H., Moryadee, S., & Miller-Hooks, E. (2018). Health care system disaster-resilience
762 optimization given its reliance on interdependent critical lifelines. *Journal of Infrastructure Systems*, 25(1):
763 04018044. [https://doi.org/10.1061/\(ASCE\)IS.1943-555X.0000465](https://doi.org/10.1061/(ASCE)IS.1943-555X.0000465).

764 Wang, J. R., Wang, J. P., Liu, M. X. & Li, Y. W. (2014). Global stability analysis of an SIR epidemic model
765 with demographics and time delay on networks. *Physica A-Statistical Mechanics & Its Applications*, 410:
766 268-275. <https://doi.org/10.1016/j.physa.2014.05.011>.

767 Wang, Y. C., Xiao, R. B. (2016). An ant colony-based resilience approach to cascading failures in cluster
768 supply network. *Physica A*, 462: 150-166. <https://doi.org/10.1016/j.physa.2016.06.058>.

769 Wells, E. M., Boden, M., Tseytlin, I. & Linkov, I. (2022) Modeling critical infrastructure resilience under
770 compounding threats: A systematic literature review. *Progress in Disaster Science*, 15: 100244.
771 <https://doi.org/10.1016/j.pdisas.2022.100244>

772 Whitman, M.G., Barker, K., Johansson, J. & Darayi, M. (2017). Component importance for multi-commodity
773 networks: Application in the Swedish railway. *Computers & Industrial Engineering*, 112: 274-288.
774 <https://doi.org/10.1016/j.cie.2017.08.004>.

775 Worldometer. (2023). Retrieved from <https://www.worldometers.info/coronavirus/>. Accessed at 12:02, Feb 28,
776 2023 (Greenwich time).

777 Xin, Y., Gao, C., Wang, Z., Zhen, X. Y., & Li, X. H. (2019). Discerning Influential Spreaders in Complex
778 Networks by Accounting the Spreading Heterogeneity of the Nodes. *IEEE Access*, 9: 92070-92078.
779 <https://doi.org/10.1109/ACCESS.2019.2927775>.

780 Zeng, Z. G., Fang, Y. P., Zhai, Q., & Du, S. (2021). A Markov reward process-based framework for resilience
781 analysis of multistate energy systems under the threat of extreme events. *Reliability Engineering &
782 System Safety*, 209(7): 107443. <https://doi.org/10.1016/j.ress.2021.107443>.

- 783 Zhang, J. P., & Jin, Z. (2011). The analysis of an epidemic model on networks. *Applied Mathematics &*
784 *Computation*, 217(17): 7053-7064. <https://doi.org/10.1016/j.amc.2010.09.063>.
- 785 Zhang, W. J., Shi, X.L., Huang, A. Q., Hua, G. W. & Teunter, R. H. (2021). Optimal stock and capital reserve
786 policies for emergency medical supplies against epidemic outbreaks, *European Journal of Operational*
787 *Research*,2021, ISSN 0377-2217. <https://doi.org/10.1016/j.ejor.2021.06.026>.
- 788 Zhao, X., Wu, C., Wang, S. & Wang, X. (2018). Reliability analysis of multi-state k-out-of-n: G system with
789 common bus performance sharing. *Computers & Industrial Engineering*, 124: 359-369.
790 <https://doi.org/10.1016/j.cie.2018.07.034>.
- 791 Zheng, J. F., Gao, Z. Y., & Zhao, X. M. (2007). Clustering and congestion effects on cascading failures of
792 scale-free networks. *EPL (Europhysics Letters)*, 79(5): 46-56. [https://doi.org/10.1209/0295-](https://doi.org/10.1209/0295-5075/79/58002)
793 [5075/79/58002](https://doi.org/10.1209/0295-5075/79/58002).
- 794 Zhou, J., Huang, N., Coit, D. W. & Felder, F. A. (2018). Combined effects of load dynamics and dependence
795 clusters on cascading failures in network systems. *Reliability Engineering and System Safety*, 2018,
796 170(1): 116-126. <https://doi.org/10.1016/j.ress.2017.10.008>.
- 797 Zou, C. C., Towsley, D. & Gong, W. (2004). Email worm modeling and defense. 13th International Conference
798 on Computer Communications and Networks (IEEE Cat. No.04EX969). [https://doi.org/doi:](https://doi.org/doi:10.1109/ICCCN.2004.1401687)
799 [10.1109/ICCCN.2004.1401687](https://doi.org/doi:10.1109/ICCCN.2004.1401687).